Differential MMP-14 targeting by Biglycan (BGN), Decorin (DCN), Fibromodulin (FMOD), and Lumican (LUM) unraveled by In Silico Approach

R Rivet, R Mallenahalli Rao, P Nizet, N Belloy, L Huber, M Dauchez, L Ramont, S Baud, S Brézillon

Differential MMP-14 targeting by Biglycan (BGN), Decorin (DCN), Fibromodulin (FMOD), and Lumican (LUM) unraveled by *In Silico* Approach

R. Rivet[1+], R. Mallenahalli Rao[1,2+], P. Nizet[1], N. Belloy[1,2], L. Huber[1], M. Dauchez[1,2], L. Ramont[1,3], S. Baud[1,2*], S. Brézillon[1*]

[1]CNRS UMR 7369, Matrice Extracellulaire et Dynamique Cellulaire (MEDyC), Université de Reims Champagne Ardenne, 51095 Reims, France. [2]P3M, Multi-Scale Molecular Modeling Platform, Université de Reims Champagne Ardenne, 51095 Reims, France. [3]CHU Reims, Service Biochimie Pharmacologie-Toxicologie, 51092 Reims, France. [+]co-first authors, *co-last authors

PURPOSE: Small leucine-rich proteoglycans (SLRPs) are major regulators of extracellular matrix assembly and cell signaling. Lumican, a member of the SLRPs family, and its derived peptides were shown to possess anti-tumor activity by interacting directly with the catalytic domain of MMP-14 leading to the inhibition of its activity. The aim of the present report was to characterize by *in silico* 3D modeling the structure and the dynamics of four SLRPs (Biglycan (BGN), Decorin (DCN), Fibromodulin (FMOD), Lumican (LUM)) including their core protein and their specific polysaccharide chains to assess their capacity to bind to MMP-14 and to regulate its activity.

METHODS: Molecular docking experiments were performed to identify the specific amino acids of MMP-14 interacting with each of the four SLRPs using the Hex software. The inhibition of each SLRP (100nM) on MMP-14 activity was measured and the constants of inhibition (K_i) were evaluated. The impact of the glycan chain number, structures and dynamics of lumican on the interaction with MMP-14 was assessed *in silico* by molecular dynamics simulations using GROMACS software.

RESULTS: Molecular docking analysis showed that all SLRPs bind to MMP-14 through their concave face, but in different regions of the catalytic domain of MMP-14. Each SLRPs inhibited significantly the MMP-14 activity (BGN: 92%, K_i: 19nM; DCN: 76%, K_i: 30.9nM; FMOD: 83%, K_i: 27.1nM; LUM: 86%, K_i: 29.3nM). Finally, molecular dynamics showed the role of glycan chains in interaction with MMP-14 and shielding effect of SLRPs.

DISCUSSION: Altogether, the results demonstrated that each SLRP exhibited inhibition of MMP-14 activity. However, the differential targeting of MMP-14 by the SLRPs was shown to be related not only to the core protein conformation but also to the glycan chain structures and dynamics.

CONCLUSION: These results might explain, at least in part, the differential effects of SLRPs in tumor progression due to the differential regulation of SLRPs on MMP-14 activity.

I. Comparisons of the human BGN, DCN, FMOD, and LUM core protein structures and post-translational modification positions

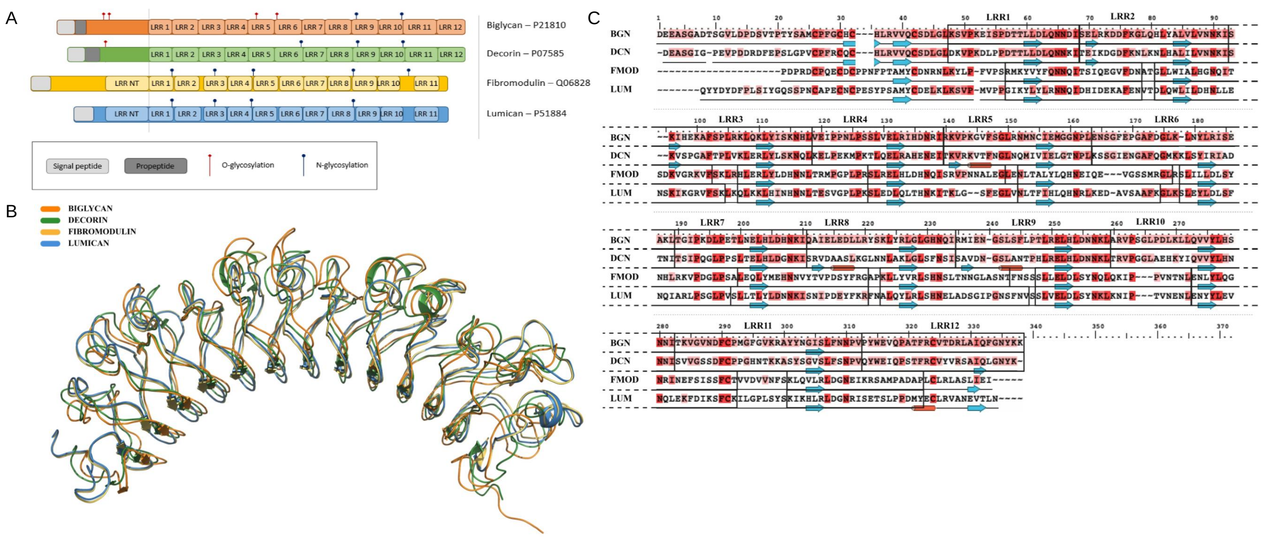

(A) Schematic comparison of the LRR sequences of BGN, DCN, FMOD and LUM from LRR1 to LRR12 and positions of their O- and N-glycosylation sites. The locations of the LRR and glycosylation sites were extracted from the uniprot server using the sequence references specified on the right of the panel. Signal peptide and propeptide are depicted. (B) Structural alignment of the four SLRP structures. (C) Dual presentation of the sequence and the local secondary structure alignment. Sequence conservation is highlighted by colored letters: pink (identity for two out of four sequences), dark red (identity for all four sequences). Elements of the local secondary structure are depicted using blue arrows (β-sheets) and red cylinders (α-helices). LRR positions are indicated as rectangular boxes.

II. Secondary structures and N-glycosylation positions on human BGN, DCN, FMOD and LUM

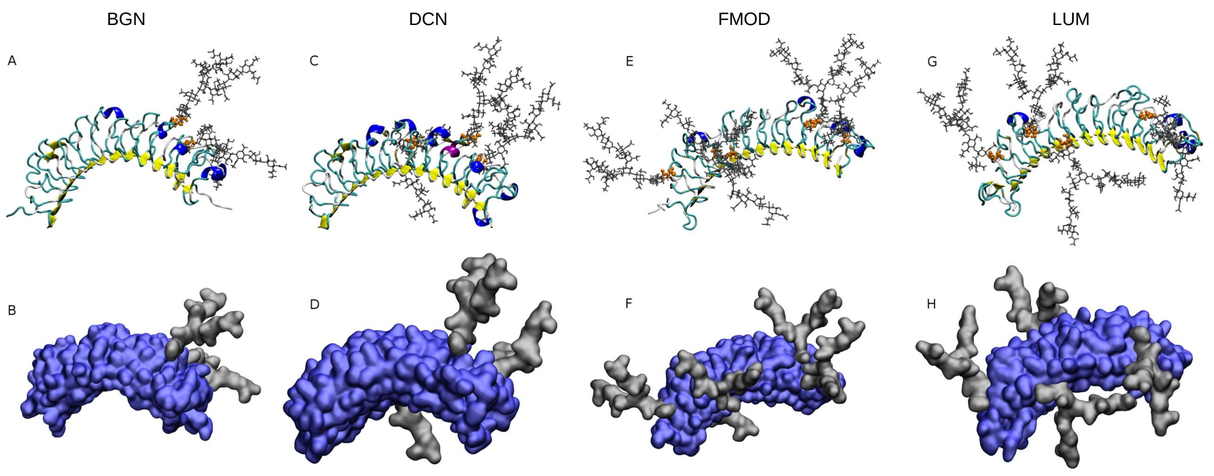

For each human SLRP, two types of representations are shown: a **cartoon representation of the backbone** (A, C, E, G) and **a surface representation** that also considers the occupancy of the side chains (B, D, F, H). The cartoon representations are colored according to the secondary structure of the core proteins and the residues bearing the N-glycosylations are displayed using orange Van der Waals motifs. Bi-antennary glycosylated chains are modeled with gray licorice (A, C, E, G) or gray surfaces (B, D, F, H).

III. MMP-14 catalytic domain complexes formed with human SLRPs

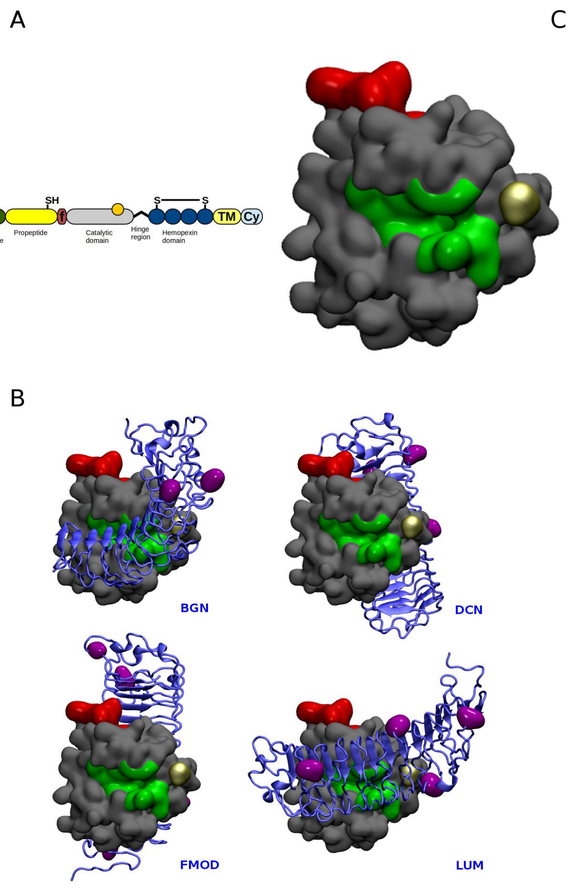

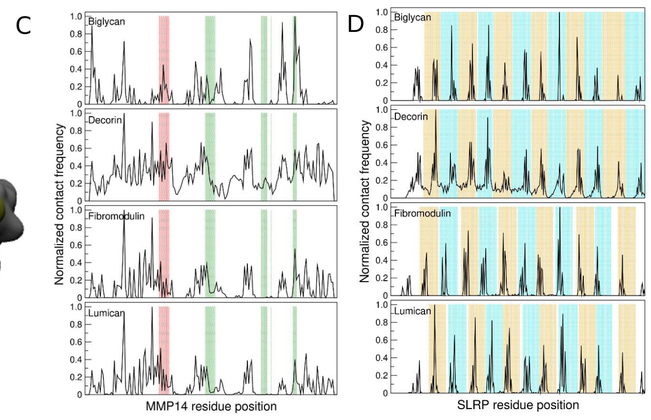

(A) **MMP-14 domain structure** and **surface representation of the catalytic domain.** The coordinates extracted from the pdb structure 1BQQ present a **catalytic pocket** and the **MT-LOOP**. The ASN229 is highlighted in orange as a possible N-glycosylation site. Adapted from Pietraszek-Gremplewicz *et al.*, Matrix Biology, 2019.

(B) **MMP-14 catalytic domain complexes** formed with **human SLRPs** (BGN, DCN, FMOD, LUM). The results were obtained with the HEX software and correspond to the best binding energy. Residues bearing the **N-glycosylations** are displayed using purple surfaces.

(C) **MMP-14 residue** positions interacting with **SLRPs** in the MT-LOOP and in the **catalytic pocket** of **MMP-14.**

(D) **SLRPs residue** positions interacting with **MMP-14.** The **LRRs** in **BGN, DCN, FMOD** and **LUM** are indicated in orange and blue, alternatively.

IV. MMP-14 activity regulated by SLRPs

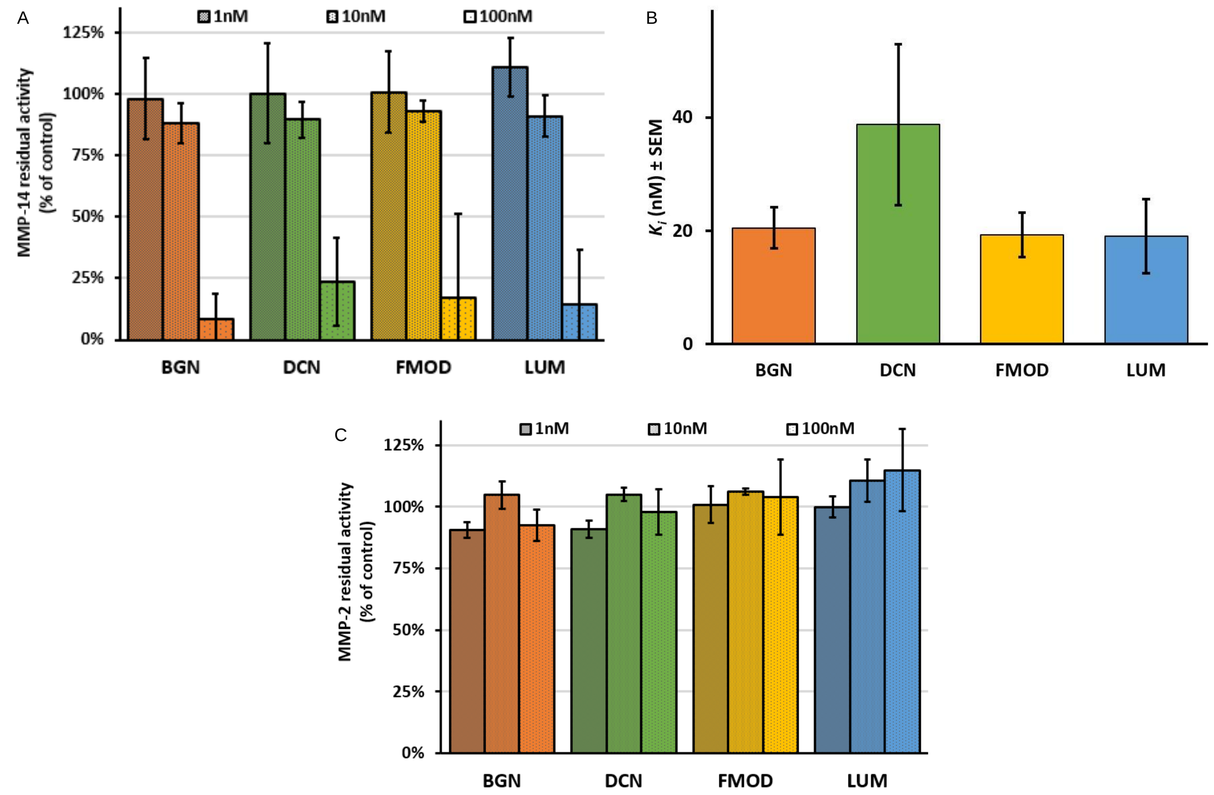

(A) Effect of biglycan (BGN), decorin (DCN), fibromodulin (FMOD), and lumican (LUM) on recombinant MMP-14 activity measured with increasing concentrations of SLRPs (1, 10, 100 nM). Data are presented as mean values ± SD from four independent experiments. (B) Measurement of the K_i for each SLRP. (C) Effect of biglycan (BGN), decorin (DCN), fibromodulin (FMOD), and lumican (LUM) on recombinant MMP-2 activity measured with increasing concentrations of SLRPs (1, 10, 100 nM). Data are presented as mean values ± SD from three independent experiments.

V. Impact of the carbohydrate shielding of lumican on LRR accessibility

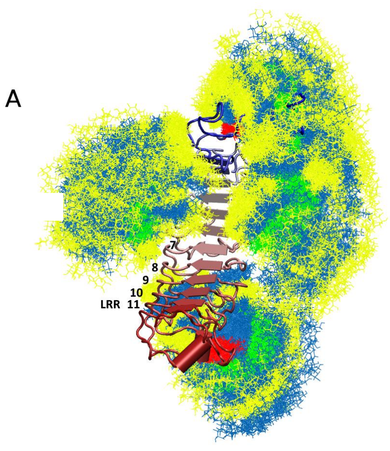

B

LRR	Residue	AccAr from MD (Å²)	RelAcc (%)	Accessibility	AccAr from starting structure (Å²)	RelAcc (%)	Accessibility
7	T209	11.9 ± 5.1	8.2	Buried	3.3	2.2	Buried
	L210	0.3 ± 1.0	0.0	Buried	0.0	0.0	Buried
	V211	35.3 ± 8.5	15.4	Buried	31.3	13.6	Buried
9	E258	47.4 ± 11.1	25.9	Accessible	63.1	34.4	Accessible
	L259	0.1 ± 0.6	0.0	Buried	0.0	0.0	Buried
	D260	17.2 ± 4.8	11.2	Buried	22.1	14.5	Buried
11	H308	41.4 ± 15.1	21.1	Accessible	39.4	20.1	Accessible
	L309	0.5 ± 1.4	0.0	Buried	0.0	0.0	Buried
	R310	75.0 ± 12.0	31.1	Accessible	92.1	38.1	Accessible

(A) **Front view showing the solvent-unaccessible as well as solvent accessible LRRs.** The C-terminal LRRs (LRR-7 to LRR-11) are labelled adjacent to the respective β-strands. (B) **Solvent accessible surface areas (AccAr) and relative accessibility (RelAcc) of selected lumican residues that are part of LRR7, LRR9 and LRR11.** A residue is considered buried when its RelAcc is < 20 and it is considered accessible when its RelAcc is > 20. >> improved accessibilities upon glycosylation

VI. Impact of the carbohydrate shielding of lumican on MMP-14 cleavage sites accessibility

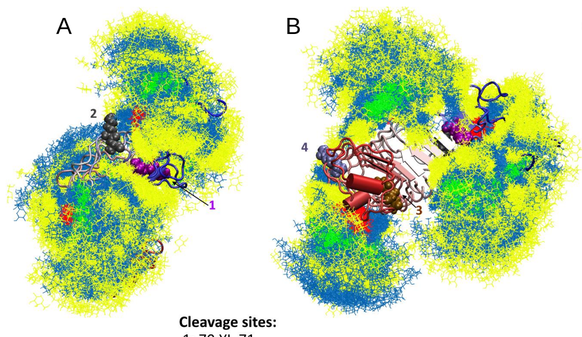

Cleavage sites:
1: 70-YL-71
2: 84-KA-85
3: 275-NL-276
4: 285-QL-286

C

Cleavage site	Residue	AccAr from MD (Å²)	RelAcc (%)	Accessibility	AccAr from starting structure (Å²)	RelAcc (%)	Accessibility
1 (in LRR 1)	Y70	38.7 ± 18.7	16.8	Buried	53.8	23.4	Accessible
	L71	0.4 ± 1.3	0.0	Buried	0.0	0.0	Buried
2 (in LRR 1)	K84	160.5 ± 2.4	75.0	Accessible	141.3	66.0	Accessible
	A85	14.9 ± 13.5	13.1	Buried	23.3	20.6	Accessible
3 (in LRR 9)	N275	65.4 ± 12.9	41.3	Accessible	84.9	53.7	Accessible
	L276	0.5 ± 1.2	0.0	Buried	0.0	0.0	Buried
4 (in LRR 10)	O285	80.0 ± 18.3	42.3	Accessible	71.9	45.5	Accessible
	L286	0.3 ± 1.0	0.0	Buried	0.0	0.0	Buried

(A) Top-view showing the N-terminal half of lumican with the residues of cleavage sites 1 and 2 represented as Van der Waals (VdW) spheres. (B) Bottom-view showing the C-terminal half of lumican with the residues of cleavage sites 3 and 4 represented as VdW spheres. Protein is represented as cartoon, coloured in blue-white-red scheme (N-terminal to C-terminal), and carbohydrate residues are represented as sticks and coloured according to the SNFG scheme [Varki, Proteomics 2009]. The cleavage sites were taken from the experimental studies on lumican proteolysis by MMP-14 [Li, Cancer Research 2004]. **(C) Solvent accessible surface areas (AccAr) and relative accessibility (RelAcc) of lumican residues situated in the cleavage sites.** A residue is considered buried when its RelAcc is < 20, and it is considered accessible when its RelAcc is > 20. >> decreased accessibilities upon glycosylation

CONCLUSIONS: The *in silico* strategy gives us prediction related to the MMP-14 biological activity with the four SLRPs. Crucial residues of the catalytic region of MMP-14 and of SLRPs could be identified. Statistical comparisons of the number of contacts could be enriched by taking into account the frequency of the SLRP conformations along MD simulations. Impact of the carbohydrate shielding of LUM on LRR accessibility and on MMP-14 cleavage sites were identified upon glycosylation.